ARTHRITIS & RHEUMATISM
Vol. 65, No. 11, November 2013, pp 2847–2856
DOI 10.1002/art.38085

Insufficient Autoantigen Presentation and Failure of Tolerance in a Mouse Model of Rheumatoid Arthritis

Jason Perera, Xiao Liu, Yuzhen Zhou, Nora E. Joseph, Liping Meng, Jerrold R. Turner, and Haochu Huang

Objective. **In the K/BxN mouse model of rheumatoid arthritis, T cells reactive for the self antigen glucose-6-phosphate isomerase (GPI) escape negative selection even though GPI expression is ubiquitous. We sought to determine whether insufficient GPI presentation could account for the failure of negative selection and for the development of arthritis.**

Methods. **To increase the antigen presentation of GPI, we generated transgenic mice expressing a membrane-bound form of GPI (mGPI) and crossed them with K/BxN mice. A monoclonal antibody specific for the α-chain of the KRN T cell receptor was generated to examine the fate of GPI-specific T cells.**

Results. **The mGPI-transgenic mice presented GPI more efficiently and showed a dramatic increase in negative selection and an inhibition of arthritis. Interestingly, thymic negative selection remained incomplete in these mice, and the escaped autoreactive T cells were anergic in the peripheral lymphoid organs, suggesting that enhanced antigen presentation also induces peripheral tolerance. Despite this apparent tolerance induction toward GPI, these mice developed a chronic wasting disease, characterized by colonic inflammation with epithelial dysplasia, as well as a dramatic reduction in Treg cells.**

Conclusion. **These data indicate that insufficient autoantigen expression or presentation results in defects of both central and peripheral tolerance in the K/BxN mice. Our findings also support the idea that insufficient autoantigen levels may underlie the development of autoimmunity.**

Negative selection requires that self antigens be properly accessed and efficiently presented to developing thymocytes (1,2). Hence, the expression levels and patterns of self antigens might affect the efficiency of clonal deletion (3,4). The relationship between serum protein levels and T cell clonal deletion has been investigated in several experimental systems. A serum concentration of hen egg lysozyme as low as 0.1 ng/ml ($10^{-11}M$) is sufficient to delete 3A9, but not 3.L2, hen egg lysozyme–specific T cells (5). In contrast, deletion of T cells specific for an Ig light chain as self antigen requires a serum concentration of >100 μg/ml ($10^{-6}M$) (6). Thus, the minimum expression level of a self antigen required for efficient negative selection varies greatly depending on the antigen and T cell receptor (TCR), most likely reflecting inherent differences in the way these self antigens gain access to the thymus and are processed by thymic antigen-presenting cells (APCs), as well as the affinity of the resulting peptide for major histocompatibility complex (MHC) molecules and the affinity of those peptide–MHC complexes for their cognate TCRs.

While these studies suggest a link between expression levels and tolerance induction, it is not well understood whether insufficient self-antigen expression and presentation contribute to defective T cell tolerance and development of autoimmunity. Lower susceptibility to type 1 diabetes mellitus in humans is associated with higher expression levels of insulin in the thymus, suggesting that higher levels of insulin in the thymus might promote negative selection of insulin-specific T cells (7).

Supported by the NIH (National Institute of Allergy and Infectious Diseases grant R01-AI-087645 to Dr. Huang). Mr. Perera's work was supported in part by the NIH (National Institute of Allergy and Infectious Diseases grant 2T32-AI-007090).

Jason Perera, BS, Xiao Liu, MS, Yuzhen Zhou, PhD (current address: University of Michigan Medical School, Ann Arbor), Nora E. Joseph, MD, Liping Meng, PhD, Jerrold R. Turner, MD, PhD, Haochu Huang, PhD: University of Chicago, Chicago, Illinois.

Mr. Perera and Ms Liu contributed equally to this work.

Address correspondence to Haochu Huang, PhD, Department of Medicine, Section of Rheumatology, Gwen Knapp Center for Lupus and Immunology Research, University of Chicago, 924 East 57th Street, R412, Chicago, IL 60637. E-mail: hhuang@bsd.uchicago.edu.

Submitted for publication August 24, 2012; accepted in revised form July 2, 2013.

Consistent with this idea, transgenic overexpression of preproinsulin 2 was shown to substantially reduce the onset and severity of type 1 diabetes mellitus in nonobese diabetic mice (8).

To explore how insufficient self-antigen presentation underlies defective central tolerance and, in turn, the development of autoimmunity, we used the K/BxN mouse model of rheumatoid arthritis caused by defective tolerance of a self-reactive transgenic TCR. K/BxN mice are generated when KRN TCR–transgenic mice on the B6 background (K/B) are crossed with NOD strain mice (9). The KRN TCR specifically recognizes a peptide of glucose-6-phosphate isomerase (GPI) presented by the NOD mouse–derived class II MHC A^{g7} molecule. Young K/BxN mice show signs of clonal deletion in the thymus; however, significant numbers of mature CD4+ T cells are observed at 3–4 weeks of age (9). Escaped KRN T cells become activated and drive B cells to produce high titers of anti-GPI antibodies, which induce arthritis in the joint by activating the complement cascade and cells of the innate immune system (10).

GPI is a ubiquitous enzyme involved in the glycolytic pathway. An important question is how KRN T cells that recognize a ubiquitous protein escape the series of elaborate mechanisms that usually ensure tolerance to self antigens. Peptides eluted from $I\text{-}A^{g7}$ on B cells include peptides from GPI (11,12); however, the specific GPI peptide that is recognized by the KRN TCR, $GPI^{282–294}$, is not among them, suggesting that GPI is not efficiently processed and presented to KRN T cells. In an earlier study, transgenic expression of G7m, a peptide mimic of $GPI^{282–294}$, showed massive thymic deletion of KRN T cells and elimination of Treg cells, but the precise fate of KRN T cells could not be tracked due to the lack of a clonotype antibody (13). Additionally, the G7m mimotope stimulates KRN T cells in vitro 10–100-fold better than the endogenous $GPI^{282–294}$ peptide. While the mimotope seems to derive most of this enhancement from increased binding to MHC molecules, some of the TCR contact residues differ from the native GPI peptide, which could possibly affect TCR avidity for the altered peptide–MHC complex.

In this study, we tested the hypothesis that insufficient processing and presentation of GPI could account for the failure of negative selection and tolerance in the K/BxN mice by increasing the antigen presentation of endogenous GPI. We generated a transgenic mouse expressing a membrane-bound form of GPI (mGPI) and a KRN TCR α-chain–specific antibody to track transgenic T cells. We showed that the presence of the mGPI transgene resulted in more efficient presentation of the GPI peptide, extensive deletion of KRN T cells in the thymus, and inhibition of the development of arthritis. Despite this greatly enhanced negative selection, KRN T cells still escape and accumulate in the periphery, yet unlike their arthritogenic counterparts, these escaped T cells are maintained in an unresponsive state towards GPI. This unresponsiveness does not appear to be mediated by Treg cells, as mGPI-transgenic mice develop much fewer thymic and splenic Treg cells compared to their non-transgenic littermates. Furthermore, this decrease in Treg cells correlates with the development of a wasting disease characterized by colonic inflammation and high-grade epithelial dysplasia. Taken together, our data indicate that insufficient autoantigen expression and presentation can affect both central and peripheral tolerance and may underlie the development of autoimmunity.

MATERIALS AND METHODS

Generation of mGPI-transgenic mice. The leader sequence from the $H\text{-}2K^b$ gene was amplified by polymerase chain reaction (PCR) from the pODpCAGGS plasmid (14) and ligated to the full-length complementary DNA (cDNA) of GPI. The joint fragment was cloned into the pODpCAGGS plasmid using *Xba* I to fuse to the $H\text{-}2D^b$ transmembrane region. The fragment without vector sequences was used to generate transgenic B6 mice by staff at the Transgenic Core Facility of the University of Chicago. Founders were identified by PCR of tail DNA using specific primers. All experiments were approved by the Institutional Animal Care and Use Committee of the University of Chicago.

Western blotting. Organs were homogenized in a tissue grinder with glass pestles (Kontes Glass) in 50 m*M* Tris HCl, pH 7.4, 150 m*M* NaCl, and 1% Nonidet P40 with a protease inhibitor cocktail (Roche). The lysates were centrifuged at 12,000*g*. The supernatant was used for the cytoplasmic fraction. The pellet (including nuclei) was dissolved in 2% sodium dodecyl sulfate, sonicated, and used for the membrane fraction. GPI was detected using serum from the K/BxN mice. The blots were stripped and reprobed with an anticlathrin heavy-chain antibody (clone 23, catalog no. 610500; BD Transduction Laboratory) and an antiactin antibody (catalog no. MAB1501R; Chemicon) for the membrane and cytoplasmic fractions, respectively.

Quantitative reverse transcription–PCR (RT-PCR). Organs were homogenized in TRIzol using a Dounce homogenizer. Following RNA purification, 1 μg of total RNA was used for cDNA synthesis by SmartScribe reverse transcriptase (Clontech).

Forward (CCACTAACGGACTGATCAGCTTCATC) and reverse (AAGAGTCAGTGGACGGAGGA) primers were designed to specifically amplify the mGPI transgene, and quantitative RT-PCR was performed using SYBR Green PCR Master Mix (Applied Biosystems). C_t values were normalized

to a standard curve of cDNA from an mGPI transgene–positive colon sample.

Enzyme-linked immunosorbent assay (ELISA). Serum titers of IgG anti-GPI were determined by ELISA. Plates were coated with 5 μg/ml of recombinant mouse GPI. Serial dilutions of serum samples were detected with the use of biotinylated goat anti-mouse IgG (subclasses 1 plus 2a plus 2b plus 3) Fcγ-specific antibody (Jackson ImmunoResearch) followed by alkaline phosphatase–conjugated streptavidin. The data were fitted by a 4-parameter curve using GraphPad Prism software. The titer was defined as the serum dilution that gave an optical density of 50% maximum (inflection point) of the curve.

T cell hybridoma and antigen presentation assay. Naive T cells from KRN-transgenic mice on the B6 background were injected into TCR$\alpha^{-/-}$/B6xNOD F1 mice to activate them. One week after injection, CD4+ T cell were purified from the host spleen and were directly fused with the BWZ.36 fusion partner (15). T cell hybrids were subcloned and screened for LacZ activity after culturing with GPI-specific B cells as APCs. Clone G2 was chosen for its high LacZ activity and low background activity.

For antigen presentation assays, 1×10^5 KRN.G2 hybridoma cells were incubated for 24 hours in 96-well plates with splenocytes from the indicated mice. Cells were lysed, and the total LacZ activity was measured using chlorophenol red β-D-galactopyranoside, a chromogenic substrate.

Primary T cell proliferation assay. Splenocytes were labeled with carboxyfluorescein succinimidyl ester (CFSE) and enriched for CD4+ cells by positive selection on magnetic columns. Labeled CD4+ splenocytes (2.5×10^4) were mixed with stimulator splenocytes from a B6xNOD F1 mouse (2.5×10^5) that had been depleted of CD4+ and CD8+ cells by negative selection on magnetic columns. Cells were cultured in complete medium for 4.5 days with graded concentrations of $GPI^{282–294}$ peptide, with or without of 25 units/ml of human interleukin-2 (IL-2; PeproTech). Cells were stained with anti-CD4, anti-KRNα, and propidium iodide and analyzed on a FACSCanto analyzer (BD Biosciences).

Antibodies and flow cytometry. Anti-KRNα antibody (clone 3-4G-B7) was generated by immunizing B6 mice with KRN T cells that also express a membrane-bound ovalbumin as carrier for T cell help (14) (details to be described in a separate article at a later date). Commercially obtained monoclonal antibodies used in these studies included anti-CD4, anti-CD8α, anti-TCR Vβ6, and anti-TCRβ (BD PharMingen). Detection of Treg cells was carried out with a FoxP3 staining kit (eBioscience). Briefly, cells were first stained with anti-CD4, anti-CD8, or anti-CD25 antibodies and were then stained intracellularly with anti-FoxP3.

Generation of bone marrow chimeric mice. T cell–depleted bone marrow cells ($1–5 \times 10^6$) were administered to lethally irradiated (1,050 rads) host mice by intravenous injection through the tail vein. Chimeric mice were analyzed 2–3 months after the bone marrow reconstitution.

RESULTS

Generation of mGPI-transgenic mice. Membrane proteins are processed and presented efficiently by class II MHC molecules, and expression of peptide in a membrane-bound form enhances its presentation (16,17). Therefore, we adapted the approach of Ehst et al (14) to express a membrane-bound form of GPI by fusing a signal peptide to the N-terminus of GPI and a membrane domain to its C-terminus. The fusion protein is driven by a ubiquitous chicken β-actin promoter and a cytomegalovirus immediate-early enhancer (Figure 1A).

Since GPI is an enzyme involved in glucose metabolism and its overexpression might have adverse effects, we mutated the histidine-388, which is critical for its enzymatic activity (18), to a glycine. This mutation does not change the GPI peptide 282–294 that is recognized by KRN T cells. The expression of the construct was first tested in cultured 293 cells. As shown in Figure 1B, surface GPI expression was readily detectable by flow cytometry.

The construct was then used to generate transgenic mice on the C57BL/6 background, and 11 founders were identified by PCR. Unexpectedly, we were not able to detect surface GPI expression in any of the founders. The lack of surface GPI expression could be due to incorrect folding, unstable configuration on the cell surface, or its quick internalization. However, surface expression is not required for efficient antigen processing and presentation (16), and expression of mGPI did target GPI to the membrane fraction of cells without affecting the endogenous, cytoplasmic GPI levels, as demonstrated by Western blot analysis (Figure 1C). One transgenic mouse line (line 5, designated as mGPI) was used in subsequent studies. Using quantitative RT-PCR, we confirmed that transgene expression in this line was detectable in all organs assayed (Figure 1E).

Increased presentation of GPI peptide in mGPI-transgenic mice. To confirm that overexpression of mGPI increased the presentation of GPI peptide, we generated a T cell hybridoma (designated KRN.G2) using T cells from KRN-transgenic mice and BWZ.36 fusion partner that carries an NF-AT-LacZ construct (15). Upon TCR engagement by the cognate peptide–MHC complex, LacZ is produced, providing a convenient and sensitive readout relative to the measurements of IL-2 production. The mGPI mice were first bred to the B6.H-2^{g7} congenic mice to introduce the I-A^{g7} molecule (referred to as $mGPI^+$/g7 mice), since KRN T cells are specific for GPI peptide presented by I-A^{g7} only. KRN.G2 hybridoma cells were cultured with splenocytes from $mGPI^+$/g7 mice or transgene-negative littermates ($mGPI^-$/g7), or as a positive control, the cells were cultured with splenocytes from the anti-GPI Ig-knockin mice on a $Rag^{-/-}$ mouse background, since they

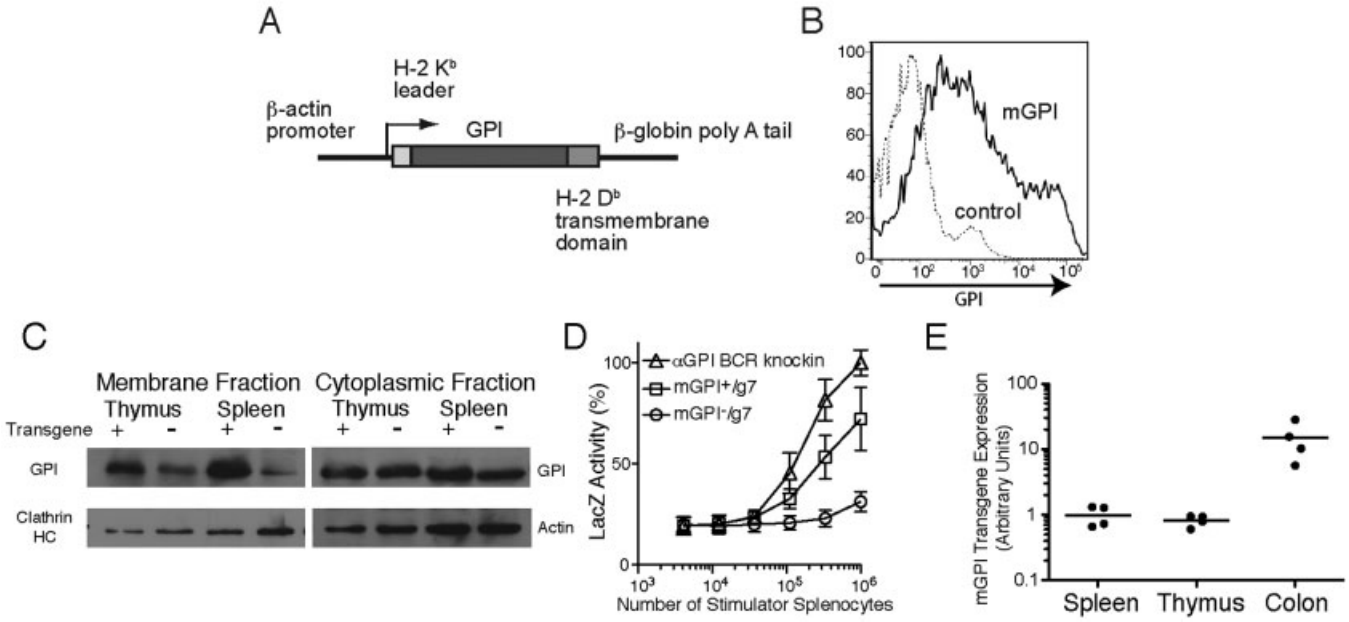

Figure 1. Generation of a membrane-bound glucose-6-phosphate isomerase (mGPI)–transgenic mouse. **A,** Map of the mGPI construct used to generate transgenic mice. **B,** Expression of mGPI on 293 cells that had been transiently transfected with the mGPI construct (solid line) by staining with an anti-GPI monoclonal antibody, as compared to mock-transfected control cells (dotted line). **C,** Subcellular distribution of mGPI. Cytoplasmic and membrane fractions from the spleen and thymus of mGPI$^+$/g7 and mGPI$^-$/g7 mice were analyzed by Western blotting. Anticlathrin heavy chain (HC) antibodies and anti–β-actin antibodies were used as loading controls for membrane and cytoplasmic fractions, respectively. The calculated molecular weights of endogenous GPI and mGPI are 62.8 kd and 67.6 kd, respectively. **D,** Capacity of splenocytes from mGPI$^+$/g7 mice to present GPI peptide. KRN.G2 hybridoma cells (1×10^5) were incubated with splenocytes from mGPI$^+$/A^{g7} mice, mGPI$^-$/A^{g7} mice, and anti-GPI B cell receptor (BCR)–knockin mice. Total LacZ activity was measured using the chromogenic substrate chlorophenol red β-D-galactopyranoside. LacZ activities were normalized to an internal control. Values are the mean $\pm$ SD of 3 independent experiments. **E,** Detection of mGPI transcript in the spleen, thymus, and colon. Real-time polymerase chain reaction analysis was performed using transgene-specific primers, and the C_t values were normalized to a standard curve of mGPI$^+$/g7 mouse colon cDNA. Each data point represents a single mouse; horizontal lines show the mean.

have a homogeneous population of GPI-specific B cells (19). The minimum number of mGPI$^+$/g7 splenocytes needed to induce LacZ was found to be 10–50-fold less than the minimum number of mGPI$^-$/g7 splenocytes needed, which verified the enhanced presentation of GPI peptide in mGPI$^+$/g7-transgenic mice (Figure 1D).

Inhibition of arthritis development by mGPI. We next crossed the mGPI$^+$/g7 mice with the KRN TCR–transgenic mice to test how arthritis development was affected by the enhanced GPI presentation. The resulting mGPI$^+$/K/g7 mice and mGPI$^-$/K/g7 littermate controls were monitored for the onset and severity of arthritis after they were weaned. As described previously (9), mGPI$^-$/K/g7 mice developed arthritis between 4 weeks and 5 weeks of age, with a sharp onset of joint swelling. Maximum ankle swelling was reached at 6–8 weeks of age, which was followed by ankle deformity. In contrast, 85% of the mGPI$^+$/K/g7 mice had no sign of arthritis. The remaining 15% of the mGPI$^+$/K/g7 mice developed mild arthritis with a delayed onset (Figure 2A).

Since arthritis is mediated by pathogenic anti-GPI antibodies, we determined the serum anti-GPI IgG antibody titers in both groups of mice. As shown in Figure 2B, the levels of IgG anti-GPI antibodies in the mGPI$^+$/K/g7 mice were ~1,000-fold lower than those in the mGPI$^-$/K/g7 mice. Thus, the blocked arthritis development in the mGPI$^+$/K/g7 mice occurs before the production of anti-GPI antibodies.

Negative selection of KRN T cells in mGPI-transgenic mice. The prevention of autoantibody production and arthritis in mGPI$^+$/K/g7 mice indicated that tolerance to GPI was restored. We analyzed the T cell compartments of these mice by flow cytometry. As described previously (9), negative selection of KRN T cells in K/BxN mice was inefficient, and significant populations of mature single-positive cells are present in the thymus and peripheral lymphoid organs. In contrast,

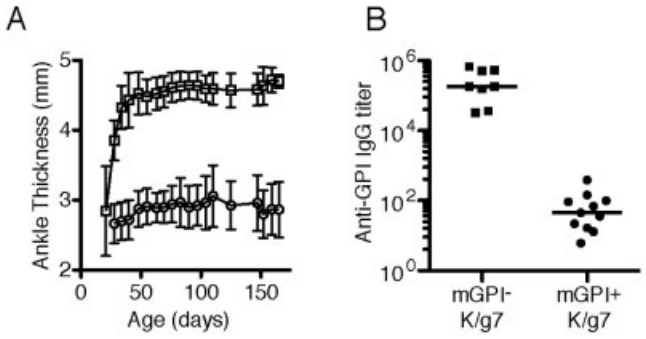

Figure 2. Effect of membrane-bound glucose-6-phosphate isomerase (mGPI) transgene on arthritis development. **A,** Ankle thickness in mGPI$^+$/K/g7 mice (circles) and in mGPI$^-$/K/g7 littermate controls (squares). Monitoring started at ~3 weeks of age. Values are the mean ± SD of 35 mGPI$^+$/K/g7 mice and 37 for mGPI$^-$/K/g7 mice. **B,** Serum titers of IgG anti-GPI in 8–12-week-old mGPI$^-$/K/g7 and mGPI$^+$/K/g7 mice. Each data point represents a single mouse; horizontal lines show the mean. Differences between groups were significant ($P < 0.001$ for each comparison, by Student's unpaired *t*-test).

thymocyte deletion in mGPI$^+$/K/g7 mice was much more effective, with a 6-fold reduction in total cellularity (Figure 3B). Analysis of the CD4/CD8 compartments showed an almost complete deletion of the double-positive (DP) thymocytes with relatively little change to the double-negative (DN) compartment, which resulted in a dramatic decrease in the ratio of DP to DN cells (Figures 3A and B). The total number of CD4+ single-positive thymocytes was decreased by 2-fold, although the percentage was increased. Despite the efficient deletion of thymocytes, there was no dramatic difference in the total number of splenocytes (mean ± SD $1.48 \pm 0.5 \times 10^8$ in mGPI$^-$/K/g7 mice and $1.75 \pm 0.7 \times 10^8$ in mGPI$^+$/K/g7 mice) and the percentage of CD4+ T cells (Figure 3A). Analysis of activation markers on CD4+ T cells from both mouse groups showed an increased proportion of CD44^{high}CD62^{low} cells, consistent with previous antigen encounter (data not shown). The increased negative selection phenotype is not dependent on the age of the animals, as mice analyzed at 2 weeks of age showed very similar results (Figure 3C).

Since allelic exclusion for the TCRα chain is not very efficient in T cells, it was not clear whether the escaping CD4+ T cells still expressed the transgene-encoded receptor or whether they instead expressed receptors produced through endogenous rearrangements. To distinguish these possibilities, we generated an antibody (clone 3-4G-B7) specific for the α-chain of the KRN TCR (Perera J, et al: unpublished data) and used it to track the fate of KRN-expressing T cells, since all of the cells that express the KRN α-chain also express the KRN β-chain. As shown in Figure 3D, 3-4G-B7 was specific for KRN+ T cells and showed no staining of wild-type T cells. The percentage of KRN+ T cells in the CD4 single-positive compartment in the thymus was reduced slightly, but the number of KRN+ T cells was reduced by 3-fold, confirming the increased deletion of KRN T cells (Figures 3C and D). Similar changes were seen in the periphery, where the percentage of

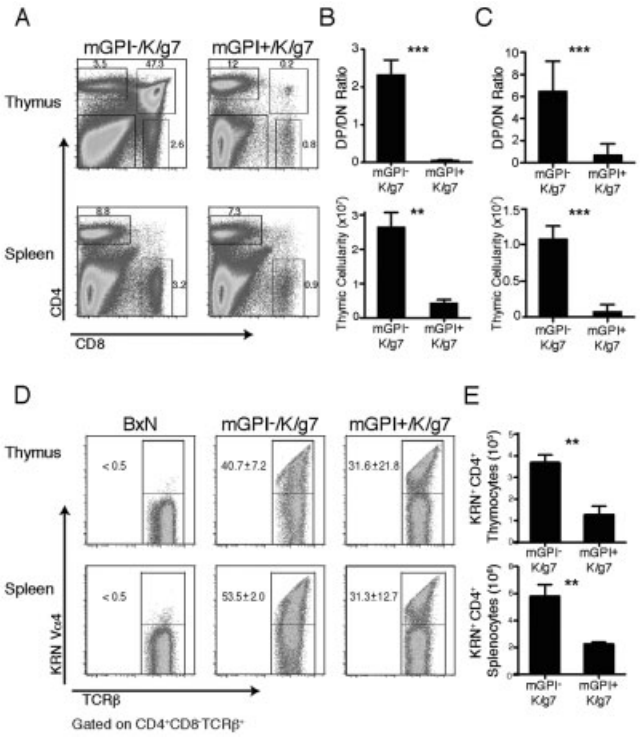

Figure 3. Selection of KRN T cells and usage of transgene-encoded T cell receptor (TCR) chains. **A,** Flow cytometry of cells prepared from the thymus or spleen of mGPI$^+$/K/g7-transgenic mice and mGPI$^-$/K/g7 littermate controls at 8–12 weeks of age. Cells were stained with anti-CD4 and anti-CD8 antibodies. Numbers represent the percentage of cells within the gate for the sample shown. **B,** Ratio of double-positive (DP) cells to double-negative (DN) cells in the thymus (top) and the number of total thymocytes (bottom) in 8–12-week-old mice (n = 5 per group and n = 8 per group, respectively). **C,** Ratio of DP cells to DN cells in the thymus (top) and the number of total thymocytes (bottom) in 2-week-old mice (n = 6 per group). **D,** Cells prepared from the thymus and spleen of B6xNOD F1 (BxN), mGPI$^-$/K/g7 control, and mGPI$^+$/K/g7-transgenic mice at 8–12 weeks of age. Cells were stained with an antibody specific for KRN TCRα (3-4G-B7) and analyzed by flow cytometry, gating first on CD4+ single-positive cells. Numbers represent the mean ± SD percentage of cells within the KRN+ gate for 5 mice. **E,** Total number of CD4+ single-positive KRN+ T cells in the thymus (top) and spleen (bottom) of mGPI$^-$/K/g7 and mGPI$^+$/K/g7 mice (n = 5 per group). Values in **B, C,** and **E** are the mean ± SD. * = $P < 0.05$; ** = $P < 0.01$; *** = $P < 0.001$, by Student's unpaired *t*-test.

KRN+ T cells among CD4+ T cells was decreased 40%, and the number of KRN+ T cells was reduced 3-fold (Figures 3D and E). These results show that despite a reduction in numbers, there is still a significant population of KRN T cells in the periphery, however, the abrogation of antibody production and arthritis indicate that these KRN T cells are functionally silenced.

We confirmed this by measuring the T cell response to $GPI^{282–294}$ peptide in vitro. CD4+ T cells from the spleens of $mGPI^{+}$/K/g7 and $mGPI^{-}$/K/g7 mice were enriched and labeled with CFSE. These labeled splenocytes were mixed with A^{g7}-bearing stimulator cells in the presence of graded amounts of $GPI^{282–294}$ peptide. KRN+CD4+ T cells from $mGPI^{-}$/K/g7 mice proliferated robustly in response to peptide, while T cells from $mGPI^{+}$/K/g7 mice did not (Figures 4A and B). In certain models of T cell anergy, the addition of exogenous IL-2 can restore proliferation (20); however, we did not observe any effect on KRN+ T cells in cultures of cells derived from $mGPI^{+}$/K/g7 mice and supplemented with IL-2 (Figure 4B). These data support the idea that the escaped KRN T cells are maintained in a state of tolerance to GPI in the peripheral immune system.

Contribution of bone marrow–derived versus non–bone marrow–derived APCs. Thymic APCs can be subdivided into radiosensitive bone marrow–derived hematopoietic cells and radioresistant non–bone marrow–derived thymic epithelial cells. Both types of cells can efficiently mediate negative selection if they have access to the antigens (21). Since the mGPI transgene was driven by a ubiquitous promoter, we compared the relative contribution of bone marrow–derived APCs versus thymic epithelial cells for the efficient clonal deletion of the KRN+ T cells observed in the transgenic $mGPI^{+}$/K/g7 mice. Four types of bone marrow–chimeric mice were generated using bone marrow donors or hosts that did or did not express the mGPI transgene (Figure 5). Chimera 4 served as the negative control, since neither the bone marrow donor nor the host carried the mGPI transgene. Chimera 1 served as the positive control since both the bone marrow donor and the host carried the mGPI transgene. In chimera 2, only the bone marrow donor carried the mGPI transgene, and in chimera 3, only the host carried the mGPI transgene.

Analyses of the numbers of total thymocytes and the ratio of DP cells to DN cells showed that either bone marrow–derived APCs or thymic epithelial cells could mediate the efficient deletion of KRN+ T cells; however, thymic epithelial cells were slightly more efficient than bone marrow–derived APCs (by comparing chimera 2 and 3). Thymic epithelial cells also induced a more dramatic reduction in the DP:DN cell ratio, suggesting that the deletion takes place at an earlier stage in thymocyte development. This is consistent with the different anatomic localization of developing thymocytes. DP cells are mostly localized in the cortex, and they will be deleted by cortical thymic epithelial cells that have a sufficient amount of peptide–MHC complex. Deletion by bone marrow–derived APCs that mainly reside in the thymic medulla will occur at a later stage in development.

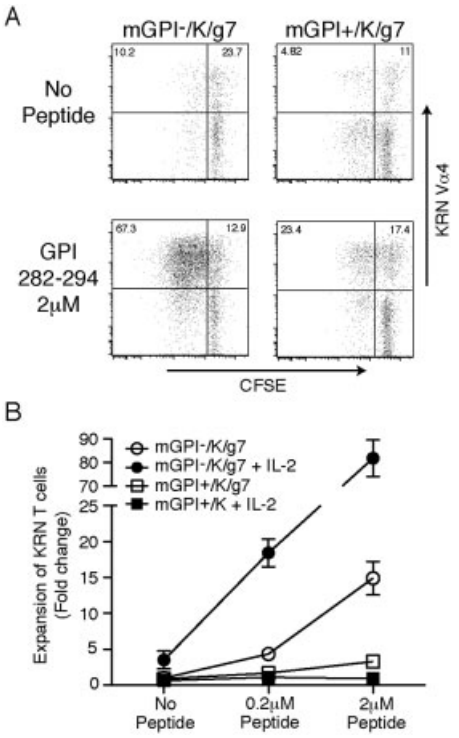

Figure 4. T cell proliferation in response to the 282–294 peptide of glucose-6-phosphate isomerase (GPI). CD4+ T cells (2.5×10^4) from $mGPI^{-}$/K/A^{g7} and $mGPI^{+}$/K/A^{g7} mice (2–5 months of age) were labeled with carboxyfluorescein succinimidyl ester (CFSE) and cocultured for 4.5 days in 96-well plates with A^{g7}-bearing stimulator cells (2.5×10^5) in the presence of graded amounts (μM) of $GPI^{282–294}$ peptide and 25 units/ml of interleukin-2 (IL-2). Individual cultures were analyzed by flow cytometry after staining with anti-CD4 and anti–KRN T cell receptor α-chain (TCRα) antibody. **A,** Representative flow cytometry plots of T cell proliferation in response to the $GPI^{282–294}$ peptide. Numbers represent the percentage of T cells that are KRN+ and have diluted CFSE (left) or remain undivided (right). **B,** Quantification of T cell proliferation relative to that in unstimulated controls. Data are shown as the fold change in the total number of KRN T cells in culture at the end of 4.5 days relative to the total number in unstimulated controls. Results are representative of 3 independent experiments. Values are the mean ± SD of triplicate wells.

Defective Treg cell production and development of wasting disease in $mGPI^{+}$/K/g7 mice. Although $mGPI^{+}$/K/g7 mice did not develop arthritis, measure-

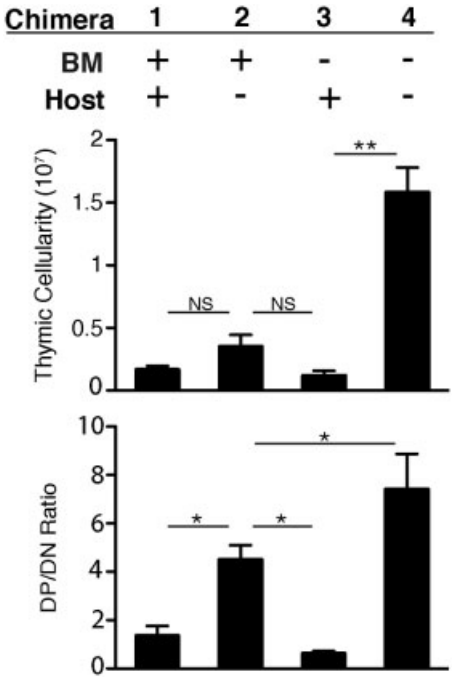

Figure 5. Contribution of bone marrow (BM)–derived antigen-presenting cells (APCs) versus non–bone marrow–derived APCs in the deletion of KRN T cells. Crisscross bone marrow chimeric mice were generated by using bone marrow donors and hosts that did (+) or did not (−) carry the membrane-bound glucose-6-phosphate isomerase transgene. Hosts were lethally irradiated (1,050 rads) before bone marrow reconstitution, and the mice were evaluated 3 months later. The numbers of total thymocytes (top) and the ratio of double-positive (DP) to double-negative (DN) cells in the thymus (bottom) are shown for each combination of bone marrow donor and host. Values are the mean ± SD of 6–12 mice per group. $* = P < 0.004$; $** = P < 0.0001$, by Student's unpaired *t*-test. NS = not significant.

ment of their body weight over time showed that their growth was arrested early (Figure 6B). By 2–3 months of age, they started to exhibit hunched posture, had ruffled fur, and were thin and lethargic. The mice that developed the most severe phenotypes were euthanized according to the guidelines of the Institutional Animal Care and Use Committee. The survival of the mice decreased with age, and by 5 months of age, only 35% of mice had survived (Figure 6A). A survey of multiple organs from these mice did not show overt inflammation in the liver, kidney, lung, heart, or pancreas. Analysis of the gastrointestinal tract of these animals revealed that the small intestine was histologically normal, but the large intestine (cecum and colon) demonstrated mild-to-severe, active, chronic inflammation in >90% of the mice analyzed at 2–5 months of age (Figure 6D). In 5 of 11 mice, low-grade epithelial dysplasia was observed, and in another mouse, high-grade dysplasia

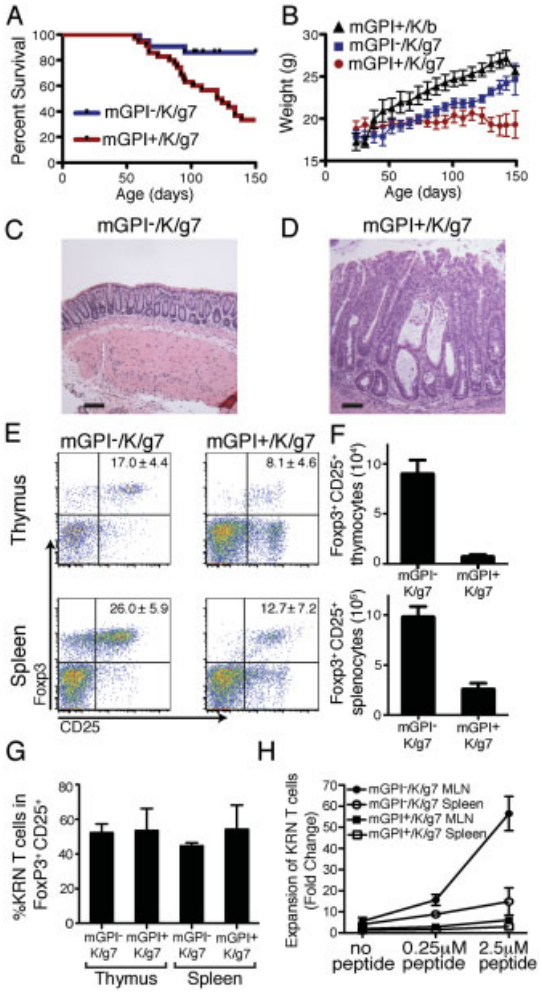

Figure 6. Wasting phenotype and loss of Treg cells in mGPI$^+$/K/g7-transgenic mice. **A,** Survival curves for mGPI$^+$/K/g7 mice (n = 31) as compared with mGPI$^-$/K/g7 mice (n = 15). Marks on the curve indicate when individual mice were removed. **B,** Changes in body weight of the mGPI$^+$/K/g7, mGPI$^-$/K/g7, and mGPI$^+$/K/b mice over time. Values are the mean ± SD of 35, 21, and 14 mice per group, respectively. **C,** Colon section from an mGPI$^-$/K/g7 control mouse showing normal histologic features. **D,** Colon section from an mGPI$^+$/K/g7 mouse showing active and chronic inflammation, with architectural distortion of crypts. Bars = 0.1 mm. **E,** Detection of Treg cells in the thymus and spleen of 8–12-week-old mGPI$^-$/K/g7 and mGPI$^+$/K/g7 mice by flow cytometry. Values are the mean ± SD percentage of Treg cells (n = 15 mice per group). **F,** Total number of FoxP3+CD25+ cells in the thymus (top) and spleen (bottom). Values are the mean ± SD of 15 mice per group. Differences between groups were significant ($P < 0.001$ for each comparison, by Student's unpaired *t*-test). **G,** Percentages of KRN-transgenic mouse T cells within the FoxP3+ Treg cell compartment, as determined with the anti-KRNα chain antibody. Values are the mean ± SD of 3 mice per group. **H,** Proliferation of KRN T cells from mesenteric lymph nodes (MLNs) and spleen in response to GPI$^{282–294}$ peptide at 6 months of age. Data are shown as the fold change in the total number of KRN T cells in culture at the end of 4.5 days relative to the total number in unstimulated controls. Results are representative of 3 independent experiments. Values are the mean ± SD of triplicate wells.

with invasion into the submucosal lining (data not shown) was noted. In contrast, we observed no colonic inflammation or dysplasia in mGPI transgene–negative mice (Figure 6C).

We next examined whether Treg cells were affected in mGPI$^+$/K/g7 mice. As shown in Figure 6E, the percentages of FoxP3+CD25+ Treg cells were greatly reduced in the thymus and spleen of mGPI$^+$/K/g7 mice. The absolute numbers of Treg cells were decreased 13.8-fold in the thymus and 3.8-fold in the spleen (Figure 6F). This reduction was not due to an inability of KRN+ T cells to be recruited into the Treg cell compartment, as KRN+ Treg cells are observed at similar frequencies in both genotypes (Figure 6G). Consistent with the role of Treg cells in suppressing intestinal autoimmunity in many experimental models (22), these data suggested that loss of Treg cells might be responsible for the development of colitis and wasting in the mGPI$^+$/K/g7 mice.

Given the unresponsive nature of KRN+ T cells in the spleen of mGPI$^+$/K/g7 mice, we sought to determine whether KRN T cells were anergic in the gut. We measured the ability of mGPI$^+$/K/g7 T cells from the mesenteric lymph nodes of 6-month-old mice to respond to GPI$^{282–294}$ peptide stimulation in vitro. While KRN+ T cells from the mesenteric lymph nodes of mGPI$^-$/K/g7 mice expanded dramatically relative to their splenic counterparts, those from mGPI$^+$/K/g7 mice remained unresponsive to peptide (Figure 6H).

DISCUSSION

In this study, we investigated whether insufficient presentation of self antigens could account for the escape of autoreactive cells from negative selection and the breakdown of tolerance in the case of a ubiquitous self antigen. In this study, we showed that enhanced presentation of GPI indeed dramatically increased KRN T cell deletion at the double-positive stage in the thymus and prevented the development of arthritis. The massive deletion in the thymus was also accompanied by significant loss of regulatory T cells and severe chronic inflammation in the colon of these transgenic animals.

Biochemical, structural, and functional analyses of the class II MHC I-A^{g7} molecule suggest that its peptide-binding properties play important roles in autoimmunity (23). In particular, I-A^{g7} binds to many of its ligands in the low micromolar range, which is weak as compared to other murine alleles, such as I-A^k, that bind to their peptides in the nanomolar range. The escape of autoreactive T cells specific for the insulin β-chain peptide (9–23) is attributed to the weak binding of the peptide to the I-A^{g7} molecule (for review, see ref. 23). Comparison of the core GPI peptide (SIALHVGFD) to the I-A^{g7} peptide binding motif (24) shows the presence of preferred amino acids at multiple positions. However, the inability to detect this peptide among those eluted from I-A^{g7} on B cells, which include other GPI peptides, supports a model in which weak binding of GPI$^{282–294}$ to I-A^{g7} allows for the escape of KRN T cells (11,12). Our results show that higher expression levels may compensate for the lower affinity of peptide for the MHC. Therefore, the efficiency of tolerance induction of a particular T cell specificity may depend on multiple factors, including the expression level of self protein, the efficiency of antigen processing and presentation, and the affinity of peptide for the MHC.

Self-antigen expression levels can affect Treg cell differentiation, although the mechanism is not well understood (for review, see refs. 25 and 26). In mGPI$^+$/K/g7 mice, increased antigen presentation leads to decreased number of Treg cells. Our results are consistent with those of previous studies in which TCR-transgenic mice specific for hemagglutinin (HA) were crossed with multiple lines of mice expressing different levels of HA (25). It was shown that the differentiation of Treg cells is dependent on the recognition of self peptide (HA peptide), since few Treg cells developed in mice expressing just the TCR transgene. Higher levels of HA expression led to more efficient deletion of cognate T cells. Of the cells that evaded deletion, similar proportions acquired FoxP3 expression. The net result was that higher expression levels of HA led to lower total numbers of Treg cells.

While the mechanism for the development of colitis in the mGPI$^+$/K/g7 mice was not addressed herein, our results are consistent with the well-established role of regulatory T cells in maintaining intestinal homeostasis (for review, see ref. 22). In the T cell–transfer model of colitis, adoptively transferred naive CD4+ T cells cause intestinal inflammation in recipient SCID mice, and colitis can be prevented by cotransferred Treg cells. The colitis in mGPI$^+$/K/g7 mice could be attributed to a decrease in Treg cell production, along with a potential narrowing of Treg cell specificities due to expression of the TCR transgene. It is also possible that KRN T cells and mGPI expression in the colon play a role in the pathogenesis of colitis. It has been demonstrated that colonic epithelial cells can aberrantly express class II MHC molecules in response to inflammation (27). The high expression of the mGPI transgene in the colon might contribute to the presen-

tation of GPI to the KRN T cells by colonic epithelial cells or other APCs, thereby exacerbating disease.

Our data support the idea that the mechanisms of both central and peripheral tolerance are important to the prevention of autoimmunity. It has been estimated that one-half to two-thirds of thymocytes that are positively selected subsequently undergo negative selection (for review, see ref. 28). However, central tolerance is neither perfect nor foolproof. In our model, there are plenty of KRN T cells in the peripheral immune system of mGPI$^+$/K/g7 mice, yet they do not initiate disease. How are they functionally silenced? Since the Treg cell numbers are significantly reduced in the mGPI$^+$/K/g7 mice, Treg cells do not appear to be responsible for the reinstatement of tolerance. Anergy is one of the major mechanisms of peripheral tolerance, and in vivo anergy has been described for several transgenic TCRs (for review, see ref. 29). Our system resembles those models in terms of the unresponsiveness of T cells and the inability of exogenous IL-2 to rescue proliferation. Studies looking at the effect of antigen expression level on in vivo anergy induction found that a pigeon cytochrome c transgene was capable of tolerizing transgenic T cells equally well at both high and low expression levels (30).

Our model is unique in two respects. First, in our model, the natural level of presentation leads to activation, and only high levels of antigen presentation lead to tolerance. Second, arthritis development provides a functional in vivo readout for T cell fate decision. It is possible that in our system, mGPI expression affects not only the strength of antigenic stimulation, but also the major type of APCs involved. In mGPI$^+$/K/g7 mice, the capacity of all B cells to present GPI is increased. It has been shown that targeting antigens to B cells could induce T cell tolerance (31–33). Further mechanistic studies are needed, and the results could shed light on the ways that autoreactive T cells escape peripheral tolerance mechanisms to drive autoimmune responses.

ACKNOWLEDGMENTS

We thank Dr. Mark Jenkins for providing the pODpCAGGS plasmid, Drs. Diane Mathis and Christophe Benoist for the KRN-transgenic mice and the B6.H-2^{g7}-congenic mice, Dr. Nilabh Shastri for providing the BWZ.36 cells, Dr. Martin Weigert for critical reading of the manuscript, and the staff at the Transgenic Core Facility of the University of Chicago for generating the mGPI-transgenic mice.

AUTHOR CONTRIBUTIONS

All authors were involved in drafting the article or revising it critically for important intellectual content, and all authors approved the final version to be published. Dr. Huang had full access to all of the data in the study and takes responsibility for the integrity of the data and the accuracy of the data analysis.

Study conception and design. Perera, Huang.

Acquisition of data. Perera, Liu, Zhou, Joseph, Meng, Turner.

Analysis and interpretation of data. Perera, Liu, Joseph, Turner, Huang.

REFERENCES

1. Goodnow CC. Multistep pathogenesis of autoimmune disease. Cell 2007;130:25–35.
2. Hogquist KA, Baldwin TA, Jameson SC. Central tolerance: learning self-control in the thymus. Nat Rev Immunol 2005;5:772–82.
3. Oehen SU, Ohashi PS, Burki K, Hengartner H, Zinkernagel RM, Aichele P. Escape of thymocytes and mature T cells from clonal deletion due to limiting tolerogen expression levels. Cell Immunol 1994;158:342–52.
4. Akkaraju S, Ho WY, Leong D, Canaan K, Davis MM, Goodnow CC. A range of CD4 T cell tolerance: partial inactivation to organ-specific antigen allows nondestructive thyroiditis or insulitis. Immunity 1997;7:255–71.
5. Haribhai D, Engle D, Meyer M, Donermeyer D, White JM, Williams CB. A threshold for central T cell tolerance to an inducible serum protein. J Immunol 2003;170:3007–14.
6. Bogen B, Dembic Z, Weiss S. Clonal deletion of specific thymocytes by an immunoglobulin idiotype. EMBO J 1993;12:357–63.
7. Pugliese A, Zeller M, Fernandez A, Zalcberg LJ, Bartlett RJ, Ricordi C, et al. The insulin gene is transcribed in the human thymus and transcription levels correlated with allelic variation at the INS VNTR-IDDM2 susceptibility locus for type 1 diabetes. Nat Genet 1997;15:293–7.
8. Jaeckel E, Lipes MA, von Boehmer H. Recessive tolerance to preproinsulin 2 reduces but does not abolish type 1 diabetes. Nat Immunol 2004;5:1028–35.
9. Kouskoff V, Korganow AS, Duchatelle V, Degott C, Benoist C, Mathis D. Organ-specific disease provoked by systemic autoimmunity. Cell 1996;87:811–22.
10. Ji H, Ohmura K, Mahmood U, Lee DM, Hofhuis FM, Boackle SA, et al. Arthritis critically dependent on innate immune system players. Immunity 2002;16:157–68.
11. Suri A, Vidavsky I, van der Drift K, Kanagawa O, Gross ML, Unanue ER. In APCs, the autologous peptides selected by the diabetogenic I-Ag7 molecule are unique and determined by the amino acid changes in the P9 pocket. J Immunol 2002;168:1235–43.
12. Dongre AR, Kovats S, deRoos P, McCormack AL, Nakagawa T, Paharkova-Vatchkova V, et al. In vivo MHC class II presentation of cytosolic proteins revealed by rapid automated tandem mass spectrometry and functional analyses. Eur J Immunol 2001;31:1485–94.
13. Shih FF, Mandik-Nayak L, Wipke BT, Allen PM. Massive thymic deletion results in systemic autoimmunity through elimination of CD4$^+$ CD25$^+$ T regulatory cells. J Exp Med 2004;199:323–35.
14. Ehst BD, Ingulli E, Jenkins MK. Development of a novel transgenic mouse for the study of interactions between CD4 and CD8 T cells during graft rejection. Am J Transplant 2003;3:1355–62.
15. Sanderson S, Shastri N. LacZ inducible, antigen/MHC-specific T cell hybrids. Int Immunol 1994;6:369–76.
16. Brooks A, Hartley S, Kjer-Nielsen L, Perera J, Goodnow CC, Basten A, et al. Class II-restricted presentation of an endogenously derived immunodominant T-cell determinant of hen egg lysozyme. Proc Natl Acad Sci U S A 1991;88:3290–4.
17. Williams CB, Vidal K, Donermeyer D, Peterson DA, White JM,

Allen PM. In vivo expression of a TCR antagonist: T cells escape central tolerance but are antagonized in the periphery. J Immunol 1998;161:128–37.
18. Graham Solomons JT, Zimmerly EM, Burns S, Krishnamurthy N, Swan MK, Krings S, et al. The crystal structure of mouse phosphoglucose isomerase at 1.6Å resolution and its complex with glucose 6-phosphate reveals the catalytic mechanism of sugar ring opening. J Mol Biol 2004;342:847–60.
19. Huang H, Kearney JF, Grusby MJ, Benoist C, Mathis D. Induction of tolerance in arthritogenic B cells with receptors of differing affinity for self-antigen. Proc Natl Acad Sci U S A 2006;103: 3734–9.
20. Beverly B, Kang SM, Lenardo MJ, Schwartz RH. Reversal of in vitro T cell clonal anergy by IL-2 stimulation. Int Immunol 1992;4:661–71.
21. Stockinger B. T lymphocyte tolerance: from thymic deletion to peripheral control mechanisms. Adv Immunol 1999;71:229–65.
22. Barnes MJ, Powrie F. Regulatory T cells reinforce intestinal homeostasis. Immunity 2009;31:401–11.
23. Suri A, Levisetti MG, Unanue ER. Do the peptide-binding properties of diabetogenic class II molecules explain autoreactivity? Curr Opin Immunol 2008;20:105–10.
24. Chang KY, Suri A, Unanue ER. Predicting peptides bound to I-Ag7 class II histocompatibility molecules using a novel expectation-maximization alignment algorithm. Proteomics 2007;7:367–77.
25. Simons DM, Picca CC, Oh S, Perng OA, Aitken M, Erikson J, et al. How specificity for self-peptides shapes the development and function of regulatory T cells. J Leukoc Biol 2010;88:1099–1107.
26. Wirnsberger G, Hinterberger M, Klein L. Regulatory T-cell differentiation versus clonal deletion of autoreactive thymocytes. Immunol Cell Biol 2010;89:45–53.
27. Kuhn R, Lohler J, Rennick D, Rajewsky K, Muller W. Interleukin-10-deficient mice develop chronic enterocolitis. Cell 1993;75: 263–74.
28. Mathis D, Benoist C. Back to central tolerance. Immunity 2004; 20:509–16.
29. Schwartz RH. T cell anergy. Annu Rev Immunol 2003;21:305–34.
30. Singh NJ, Schwartz RH. The strength of persistent antigenic stimulation modulates adaptive tolerance in peripheral CD4+ T cells. J Exp Med 2003;198:1107–17.
31. Eynon EE, Parker DC. Small B cells as antigen-presenting cells in the induction of tolerance to soluble protein antigens. J Exp Med 1992;175:131–8.
32. Fuchs EJ, Matzinger P. B cells turn off virgin but not memory T cells. Science 1992;258:1156–9.
33. Yan J, Mamula MJ. B and T cell tolerance and autoimmunity in autoantibody transgenic mice. Int Immunol 2002;14:963–71.